Inorganic Chemistry
Article

*Inorg. Chem.* **2010**, *49*, 2541–2549 **2541**
DOI: 10.1021/ic100001x

# Promotive Effect of the Platinum Moiety on the DNA Cleavage Activity of Copper-Based Artificial Nucleases

**Xindian Dong,[†] Xiaoyong Wang,*[,‡] Miaoxin Lin,[†] Hui Sun,[†] Xiaoliang Yang,[†] and Zijian Guo*[,†]**

[†]*State Key Laboratory of Coordination Chemistry, School of Chemistry and Chemical Engineering,*
[‡]*State Key Laboratory of Pharmaceutical Biotechnology, School of Life Sciences, Nanjing University, Nanjing 210093, People's Republic of China*

Received January 1, 2010

Copper-based artificial metallonucleases are likely to satisfy more biomedical requirements if their DNA cleavage efficiency and selectivity could be further improved. In this study, two copper(II) complexes, $[CuL^1Cl_2]$ (**1**) and $[CuL^2Cl_2]$ (**2**), and two copper(II)−platinum(II) heteronuclear complexes, $[CuPtL^1(DMSO)Cl_4]$ (**3**) and $[CuPtL^2(DMSO)Cl_4]$ (**4**), were synthesized using two bifunctional ligands, *N*-[4-(2-pyridylmethoxy)benzyl]-*N*,*N*-bis(2-pyridylmethyl)amine ($L^1$) and *N*-[3-(2-pyridylmethoxy)benzyl]-*N*,*N*-bis(2-pyridylmethyl)amine ($L^2$). These complexes have been characterized by elemental analysis, electrospray ionization mass spectrometry, IR spectroscopy, and UV−vis spectroscopy. The DNA binding ability of these complexes follows an order of **1** < **2** < **3** < **4**, as revealed by the results of spectroscopy and agarose gel electrophoresis studies. Their cleavage activity toward supercoiled pUC19 plasmid DNA is prominent at micromolar concentration levels in the presence of ascorbic acid. The introduction of a platinum(II) center to the copper(II) complexes induces a significant enhancement in cleavage activity as compared with copper(II) complexes alone. These results show that the presence of a platinum(II) center in copper(II) complexes strengthens both their DNA binding ability and DNA cleavage efficiency.

## Introduction

Artificial nucleases have attracted much attention in view of their diverse applications as potential chemotherapeutic agents in medicine and useful cleaving reagents in molecular biology.[1−3] Transition-metal complexes constitute a rich resource for the exploration of such nucleases because of their structural and functional varieties.[4,5] Copper complexes are particularly attractive and most studied because of their biologically accessible redox potential and relatively high affinity for nucleobases.[6,7] In the presence of a reductant and dioxygen, copper complexes exert cleavage activity by generating reactive oxygen species (ROS) that oxidize DNA and lead to strand cleavage or base modification.[8,9] However, many copper(II) complexes cleave DNA randomly and possess only limited enzymatic activity.[10,11] Therefore, the development of artificial nucleases with improved efficiency and selectivity is in high demand. A number of natural nucleases require multinuclear metal centers to achieve a synergistic effect in the process of substrate recognition and scission.[12] We and others have demonstrated the synergistic effect between multicopper(II) centers in previous DNA cleavage studies.[13−16] Nevertheless, designing copper-based artificial nucleases with specific and selective DNA cleavage properties is still full of challenges.

*To whom correspondence should be addressed. E-mail: boxwxy@nju.edu.cn (X.W.), zguo@nju.edu.cn (Z.G.).

(1) Mancin, F.; Scrimin, P.; Tecilla, P.; Tonellato, U. *Chem. Commun.* **2005**, 2540–2548.
(2) Xu, Y.; Suzuki, Y.; Lönnberg, T.; Komiyama, M. *J. Am. Chem. Soc.* **2009**, *131*, 2871–2874.
(3) Tseng, T.-S. A.; Burstyn, J. N. *Chem. Commun.* **2008**, 6209–6211.
(4) Parkin, G. *Chem. Rev.* **2004**, *104*, 699–767.
(5) Jiang, Q.; Xiao, N.; Shi, P. F.; Zhu, Y. G.; Guo, Z. J. *Coord. Chem. Rev.* **2007**, *251*, 1951–1972.
(6) Chen, J. W.; Wang, X. Y.; Shao, Y.; Zhu, J. H.; Zhu, Y. G.; Li, Y. Z.; Xu, Q.; Guo, Z. J. *Inorg. Chem.* **2007**, *46*, 3306–3312.
(7) González-Álvarez, M.; Alzuet, G.; Borrás, J.; Pitié, M.; Meunier, B. *J. Biol. Inorg. Chem.* **2003**, *8*, 644–652.
(8) Thyagarajan, S.; Murthy, N. N.; Sarjeant, A. A. N.; Karlin, K. D.; Rokita, S. E. *J. Am. Chem. Soc.* **2006**, *128*, 7003–7008.
(9) Frey, S. T.; Sun, H. H. J.; Murthy, N. N.; Karlin, K. D. *Inorg. Chim. Acta* **1996**, *242*, 329–338.
(10) Maheswari, P. U.; Lappalainen, K.; Sfregola, M.; Barends, S.; Gamez, P.; Turpeinen, U.; Mutikainen, I.; van Wezel, G. P.; Reedijk, J. *Dalton Trans.* **2007**, 3676–3683.
(11) Dhar, S.; Reddy, P. A. N.; Nethaji, M.; Mahadevan, S.; Saha, M. K.; Chakravarty, A. R. *Inorg. Chem.* **2002**, *41*, 3469–3476.
(12) Liu, C. L.; Wang, M.; Zhang, T. L.; Sun, H. Z. *Coord. Chem. Rev.* **2004**, *248*, 147–168.
(13) Zhao, Y. M.; Zhu, J. H.; He, W. J.; Yang, Z.; Zhu, Y. G.; Li, Y. Z.; Zhang, J. F.; Guo, Z. J. *Chem.—Eur. J.* **2006**, *12*, 6621–6629.
(14) Tu, C.; Shao, Y.; Gan, N.; Xu, Q.; Guo, Z. J. *Inorg. Chem.* **2004**, *43*, 4761–4766.
(15) Humphreys, K. J.; Karlin, K. D.; Rokita, S. E. *J. Am. Chem. Soc.* **2002**, *124*, 6009–6019.
(16) Humphreys, K. J.; Karlin, K. D.; Rokita, S. E. *J. Am. Chem. Soc.* **2002**, *124*, 8055–8066.


Published on Web 02/01/2010

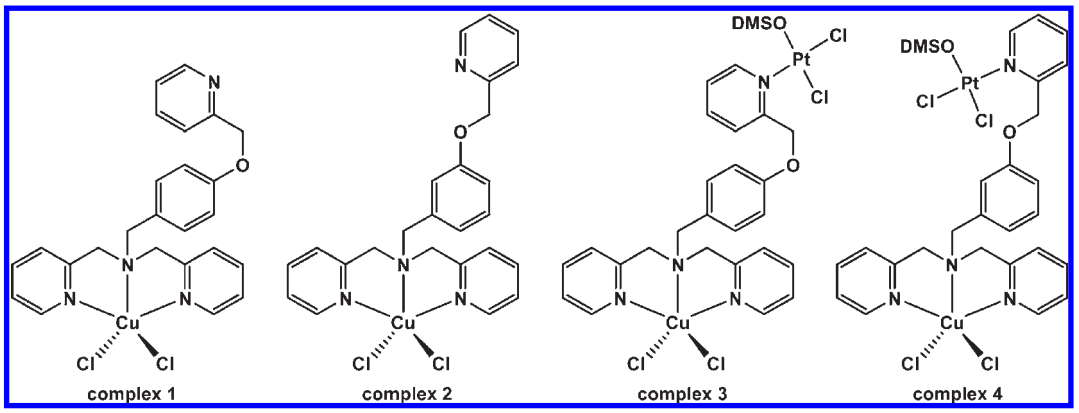


**Figure 1.** Chemical structures of complexes **1**−**4**.

It is well-known that cisplatin-type complexes bind preferentially to the GG or AG site of DNA.[17] Such a DNA sequence preference could be used as a targeting element to direct a nuclease moiety to specific DNA sites. In fact, Reedjik and co-workers have reported recently that platinated copper(3-Clip-Phen) complexes exhibited higher DNA cleavage efficiency than the copper(II) complexes alone.[18−20] However, comparisons were made on complexes with different ligands.[21] We have shown that the DNA cleavage activity of copper complexes could be largely affected by the ligand structure;[13,22] therefore the influence of the ligand should not be excluded while the effect of the platinum(II) center is discussed.

In this work, we have designed two similar ligands ($L^1$ and $L^2$), where rigid *p*-cresol or *m*-cresol is used to connect two coordination centers composed of bis(2-pyridylmethyl)amine (BPA) and 2-methylpyridine, respectively. These ligands allow us to make direct comparisons on the DNA binding and cleavage activity of both monocopper(II) and copper(II)−platinum(II) complexes (Figure 1). The effect of the platinum(II) center on the cleavage activity in **3** and **4** can be clearly illustrated by their comparison with **1** and **2**.

## Experimental Section

**Materials and Characterization.** Reagents such as $CuCl_2 \cdot 2H_2O$, *p*-cresol, *m*-cresol, and 2-(chloromethyl)pyridine hydrochloride were of analytical grade and used without further purification. Supercoiled pUC19 plasmid DNA and 5′-FAM-end-labeled 18mer DNA were purchased from TaKaRa Biotechnology (Dalian). Calf thymus DNA (CT-DNA), tris(hydroxymethyl)aminomethane (Tris), and ethidium bromide (EB) were purchased from Sigma. The electrospray ionization mass spectrometry (ESI-MS) spectra were recorded using an LCQ fleet ESI-MS spectrometer (Thermo Scientific), and the isotopic distribution patterns of the observed species were simulated using the *Isopro 3.0* program. Far-IR spectra were recorded on a Nexus 870 FT-IR spectrometer as KBr pellets (600−100 $cm^{-1}$). Elemental analysis was performed on a Perkin-Elmer 240C analytical instrument. UV−vis spectra were determined on a Shimadzu UV 3600 (UV−vis−near-IR) spectrophotometer. The $^1H$ and $^{13}C$ NMR spectra were acquired on a Bruker DRX-500 spectrometer at 298 K. The circular dichroism (CD) experiments were performed on a Jasco J-810 spectropolarimeter. Fluorescence spectra were recorded on a Perkin-Elmer LS55 luminescence spectrometer in a wavelength range of 530−780 nm with 4 nm slits for both excitation and emission at room temperature. Fluorescence imaging was performed with a Gel Doc XR (BioRad), and quantification analysis was performed with *Quantity One* software (version 4.6.2).

**Preparation of Ligands $L^1$ and $L^2$.** The intermediate 4-(bromomethyl)phenyl acetate was prepared according to the literature method with some modifications.[23] Briefly, *p*-cresol (30.00 g, 277.78 mmol) in acetic anhydride/pyridine (1:1, 80 mL) was stirred at room temperature for 48 h. *p*-Tolyl acetate was obtained after removal of the solvent. Bp: 120 °C. $^1H$ NMR ($CDCl_3$, 500 MHz, ppm): 2.31 (s, 3H, $-CH_3$), 2.37 (s, 3H, $-CH_3$), 6.98−7.00 (d, 2H, Ph−H), 7.19−7.21(d, 2H, Ph−H). $^{13}C$ NMR ($CDCl_3$, 500 MHz, ppm): 20.72, 20.91, 121.22, 129.86, 135.31, 148.53, 169.48. This ester (5.70 g, 38.00 mmol) was brominated with *N*-bromosuccinimide (9.60 g, 53.90 mmol) and benzoyl peroxide (0.28 g) in $CCl_4$ (80 mL). The exothermic reaction completed automatically after the initial heating. The mixture was filtered, and the solvent was removed to give a crude product, which was chromatographed on silica gel (petroleum ether/ethyl acetate, 10:1, v/v), and the intermediate was obtained. $^1H$ NMR ($CDCl_3$, 500 MHz, ppm): 2.32 (s, 3H, $-CH_3$), 4.51 (s, 2H, $-CH_2$), 7.08−7.10 (d, 2H, Ph−H), 7.42−7.43 (d, 2H, Ph−H). $^{13}C$ NMR ($CDCl_3$, 500 MHz, ppm): 21.15, 32.76, 122.01, 130.28, 135.41, 150.67, 169.25. *m*-Tolyl acetate and 3-(bromomethyl)phenyl acetate were prepared in a similar way except that *m*-cresol was used in the reaction instead of *p*-cresol. $^1H$ NMR ($CD_3OD$, 500 MHz, ppm): 2.26 (s, 3H, $-CH_3$), 2.32 (s, 3H, $-CH_3$), 6.91−6.93 (d, 1H, Ph−H), 6.95 (s, 1H, Ph−H), 7.07−7.08 (d, 1H, Ph−H), 7.28−7.31 (t, 1H, Ph−H). $^{13}C$ NMR ($CDCl_3$, 500 MHz, ppm): 21.07, 21.28, 118.57, 122.22, 126.65, 129.17, 139.60, 150.75, 169.53. $^1H$ NMR ($CD_3OD$, 500 MHz, ppm): 2.29 (s, 3H, $-CH_3$), 4.57 (s, 2H, $-CH_2$), 7.05−7.06 (d, 1H, Ph−H), 7.19 (s, 1H, Ph−H), 7.30−7.32 (d, 1H, Ph−H), 7.36−7.39 (m, 1H, Ph−H). $^{13}C$ NMR ($CDCl_3$, 500 MHz, ppm): 21.10, 32.56, 121.68, 122.28, 126.41, 129.78, 139.34, 150.87, 169.19.

4-[[Bis(2-pyridylmethyl)amino]methyl]phenyl acetate was prepared as follows. *N*,*N*-Diisopropylethylamine (DIEA; 2.35 g) and bis(2-pyridylmethyl)amine (BPA; 3.54 g, 17.78 mmol)[24] were added to the $CHCl_3$ solution of 4-(bromomethyl)phenyl acetate

(17) Jung, Y.; Lippard, S. J. *Chem. Rev.* **2007**, *107*, 1387–1407.
(18) de Hoog, P.; Boldron, C.; Gamez, P.; Sliedregt-Bol, K.; Roland, I.; Pitié, M.; Kiss, R.; Meunier, B.; Reedijk, J. *J. Med. Chem.* **2007**, *50*, 3148–3152.
(19) de Hoog, P.; Pitié, M.; Amadei, G.; Gamez, P.; Meunier, B.; Kiss, R.; Reedijk, J. *J. Biol. Inorg. Chem.* **2008**, *13*, 575–586.
(20) Özalp-Yaman, Ş.; de Hoog, P.; Amadei, G.; Pitié, M.; Gamez, P.; Dewelle, J.; Mijatovic, T.; Meunier, B.; Kiss, R.; Reedijk, J. *Chem.—Eur. J.* **2008**, *14*, 3418–3426.
(21) Pitié, M.; Sudres, B.; Meunier, B. *Chem. Commun.* **1998**, 2597–2598.
(22) Chen, Z. F.; Wang, X. Y.; Li, Y. Z.; Guo, Z. J. *Inorg. Chem. Commun.* **2008**, *11*, 1392–1396.
(23) Karlin, K. D.; Cohen, B. I.; Hayes, J. C.; Farooq, A.; Zubieta, J. *Inorg. Chem.* **1987**, *26*, 147–153.
(24) Matouzenko, G. S.; Bousseksou, A.; Lecocq, S.; van Koningsbruggen, P. J.; Perrin, M.; Kahn, O.; Collet, A. *Inorg. Chem.* **1997**, *36*, 2975–2981.

(4.09 g, 17.87 mmol, 30 mL) successively. The mixture was stirred for 2 days, and the resulting DIEA salt was eliminated by filtration. After removal of the solvent from the filtrate and purification by silica gel chromatography (ethyl acetate/methanol, 30:1, v/v), 4-[[bis(2-pyridylmethyl)amino]methyl]phenyl acetate was obtained. Yield: 60%. $^1$H NMR (DMSO-$d_6$, 500 MHz, ppm): 2.26 (s, 3H, $-CH_3$), 3.65 (s, 2H, $-CH_2$), 3.73 (s, 4H, $-CH_2$), 7.08−7.10 (d, 2H, Ph−H), 7.26−7.28 (m, 2H, Py−H), 7.44−7.46 (d, 2H, Ph−H), 7.58−7.60 (d, 2H, Py−H), 7.79−7.82 (m, 2H, Py−H), 8.50−8.51 (d, 2H, Py−H). $^{13}$C NMR ($CDCl_3$, 500 MHz, ppm): 21.20, 57.94, 60.11, 121.46, 122.08, 122.92, 129.80, 136.51, 136.70, 149.12, 149.83, 159.72, 169.53. ESI-MS ($m/z$) found (calcd) for $C_{21}H_{21}N_3O_2$ (M): $[M + H]^+$, 348.42 (348.17); $[M + Na]^+$, 370.33 (370.15). This intermediate (2.81 g, 8.08 mmol) and 2-(chloromethyl)pyridine hydrochloride (3.00 g, 18.46 mmol) were dissolved in anhydrous acetonitrile (30 mL), and $K_2CO_3$ (5.00 g, 36.23 mmol) was added to the solution. The mixture was heated at 65 °C for 48 h under a nitrogen atmosphere. After filtration and removal of the solvent, the brown-yellow residue was purified with chromatography (ethyl acetate/ethanol, 20:1, v/v), and light-yellow *N*-[4-(2-pyridylmethoxy)benzyl]-*N*,*N*-bis(2-pyridylmethyl)amine ($L^1$) was obtained. Yield: 40%. $^1$H NMR (DMSO-$d_6$, 500 MHz, ppm): 3.57 (s, 2H, $-CH_2$), 3.70 (s, 4H, $-CH_2$), 5.16 (s, 2H, $-CH_2$), 6.99−7.01 (d, 2H, Ph−H), 7.25−7.27 (m, 2H, Py−H), 7.33−7.35 (m, 2H, Ph−H; 1H, Py−H), 7.50−7.52 (d, 1H, Py−H), 7.57−7.59 (d, 2H, Py−H), 7.78−7.81 (m, 2H, Py−H), 7.81−7.85 (m, 1H, Py−H), 8.49−8.50 (d, 2H, Py−H), 8.57−8.58 (d, 1H, Py−H). $^{13}$C NMR (DMSO-$d_6$, 500 MHz, ppm): 57.27, 59.41, 70.85, 115.05, 122.12, 122.57, 122.99, 123.64, 130.40, 131.39, 137.03, 137.41, 149.20, 149.51, 157.25, 157.76, 159.59. ESI-MS ($m/z$) found (calcd) for $C_{25}H_{24}N_4O$ (M): $[M + H]^+$, 397.25 (397.20); $[M + Na]^+$, 419.33 (419.18); $[2M + Na]^+$, 814.92 (815.38).

The intermediate 3-[[bis(2-pyridylmethyl)amino]methyl]phenol was prepared by adding DIEA (1.60 g) and BPA (1.99 g, 10.00 mmol) to the $CHCl_3$ solution of 3-(bromomethyl)phenyl acetate (2.29 g, 10.00 mol, 30 mL) and stirring for 2 days. The precipitate of DIEA salt was removed by filtration, and the solvent in the filtrate was evaporated. The resulting oil was stirred with distilled water (100 mL), methanol (100 mL), and NaOH (50 mL, 40%) for 12 h, and then the resulting mixture was neutralized with HCl (37%). The mixture was extracted with $CHCl_3$, and the extraction was dried with $Na_2SO_4$. The solvent was removed, and the crude product was purified by $SiO_2$ column chromatography (ethyl acetate/ethanol, 20:1, v/v). $^1$H NMR (DMSO-$d_6$, 500 MHz, ppm): 3.54 (s, 2H, $-CH_2$), 3.70 (s, 4H, $-CH_2$), 6.65−6.66 (d, 1H, Ph−H), 6.82−6.83 (d, 1H, Ph−H), 6.88 (s, 1H, Ph−H), 7.11−7.14 (m, 1H, Ph−H), 7.24−7.26, (m, 2H, Py−H), 7.58−7.60 (d, 2H, Py−H), 7.77−7.81 (m, 2H, Py−H), 8.49−8.50 (d, 2H, Py−H), 9.38 (s, 1H, OH−H). $^{13}$C NMR ($CD_3OD$, 500 MHz, ppm): 58.35, 59.25, 113.89, 115.32, 119.79, 122.36, 123.29, 128.99, 137.25, 139.95, 147.96, 157.24, 159.24. ESI-MS ($m/z$) found (calcd) for $C_{19}H_{19}N_3O$ (M): $[M + H]^+$, 306.50 (306.16); $[M + Na]^+$, 328.33 (328.14). The obtained intermediate (1.80 g, 5.90 mmol) and 2-(chloromethyl)pyridine hydrochloride (2.20 g, 13.41 mmol) were dissolved in anhydrous dimethylformamide (DMF; 30 mL), and $K_2CO_3$ (5.00 g, 36.23 mmol) was added to the solution. The mixture was heated at 65 °C for 48 h under a nitrogen atmosphere. After filtration and removal of DMF, the brown-yellow residue was purified with chromatography (ethyl acetate/ethanol, 20:1, v/v), and light-yellow *N*-[3-(2-pyridylmethoxy)benzyl]-*N*,*N*-bis(2-pyridylmethyl)-amine ($L^2$) was obtained. Yield: 40%. $^1$H NMR (DMSO-$d_6$, 500 MHz, ppm): 3.59 (s, 2H, $-CH_2$), 3.70 (s, 4H, $-CH_2$), 5.19 (s, 2H, $-CH_2$), 6.91−6.92 (d, 1H, Ph−H), 6.98−7.00 (d, 1H, Ph−H), 7.09 (s, 1H, Ph−H), 7.24−7.27 (m, 2H, Py−H; 1H, Ph−H), 7.34−7.37, (m, 1H, Py−H), 7.50−7.51 (d, 1H, Py−H), 7.53−7.54 (d, 2H, Py−H), 7.77−7.80 (m, 2H, Py−H), 7.81−7.84 (m, 1H, Py−H), 8.49−8.50 (d, 2H, Py−H), 8.60−8.61 (d, 1H, Py−H). $^{13}$C NMR (DMSO-$d_6$, 500 MHz, ppm): 57.83, 59.61, 70.78, 113.95, 115.30, 121.67, 122.04, 122.58, 122.90, 123.35, 129.79, 137.21, 137.55, 141.03, 149.27, 149.57, 157.34, 158.73, 159.65. ESI-MS ($m/z$) found (calcd) for $C_{25}H_{24}N_4O$ (M): $[M + H]^+$, 397.33 (397.20); $[M + Na]^+$, 419.33 (419.18).

**Synthesis of the Complexes.** Complex **1** was prepared by mixing methanol solutions of $CuCl_2 \cdot 2H_2O$ (18.80 mg, 0.11 mmol, 1 mL) and $L^1$ (39.90 mg, 0.10 mmol, 3 mL) and stirring at room temperature for 12 h. Ether was added to the mixture, the resulting precipitate was filtered and washed with acetone and ether, and **1** was thus obtained. Yield: 90%. Elem anal. Found (calcd) for $C_{25}H_{24}ON_4Cl_2Cu$: C, 56.73 (56.55); H, 4.59 (4.56); N, 10.23 (10.55). IR (KBr pellet): $\nu_{Cu-Cl}$ 267.2 cm$^{-1}$. UV−vis [$H_2O$; $\lambda_{max}$, nm ($\varepsilon$, M$^{-1}$ cm$^{-1}$)]: 260 (12 500), 650 (85). Complex **2** was prepared in the same way but using $L^2$ as the ligand. Yield: 94%. Elem anal. Found (calcd) for $C_{25}H_{24}ON_4Cl_2Cu$: C, 56.70 (56.55); H, 4.77 (4.56); N, 10.16 (10.55). IR (KBr pellet): $\nu_{Cu-Cl}$ 274.8 cm$^{-1}$. UV−vis [$H_2O$; $\lambda_{max}$, nm ($\varepsilon$, M$^{-1}$ cm$^{-1}$)]: 260 (12 000), 651 (75).

Complex **3** was synthesized on the basis of complex **1**. *cis*-$[Pt(DMSO)_2Cl_2]$[25] (28.60 mg, 0.067 mmol) was dissolved in methanol/acetonitrile (1:6, v/v; 3 mL) and added to the methanol solution of **1** (33.00 mg, 0.063 mmol, 5 mL). The mixture was stirred at 44 °C for 48 h in the dark. Ether was added to the mixture, and the resulting product was filtered and washed with acetone and ether, which gave rise to **3**. Yield: 93%. Elem anal. Found (calcd) for $C_{27}H_{30}O_2N_4Cl_4SCuPt$: C, 37.12 (37.06); H, 3.48 (3.46); N, 6.34 (6.40). IR (KBr pellet): $\nu_{Pt-S}$ 438.3, $\nu_{Pt-Cl}$ 334.6, $\nu_{Pt-Cl}$ 311.9, $\nu_{Cu-Cl}$ 270.1 cm$^{-1}$. UV−vis [$H_2O$; $\lambda_{max}$, nm ($\varepsilon$, M$^{-1}$ cm$^{-1}$)]: 260 (14 500), 652 (90). Complex **4** was similarly prepared except that **2** was used as one of the reactants. Yield: 86%. Elem anal. Found (calcd) for $C_{27}H_{30}O_2N_4Cl_4SCuPt$: C, 37.19 (37.06); H, 3.60 (3.46); N, 6.30 (6.40). IR (KBr pellet): $\nu_{Pt-S}$ 440.4, $\nu_{Pt-Cl}$ 339.9, $\nu_{Pt-Cl}$ 312.7, $\nu_{Cu-Cl}$ 273.8 cm$^{-1}$. UV−vis [$H_2O$; $\lambda_{max}$, nm ($\varepsilon$, M$^{-1}$ cm$^{-1}$)]: 259 (12 100), 650 (75).

**DNA Binding Studies.** The stock solution of CT-DNA was prepared with a buffer (5 mM Tris-HCl/50 mM NaCl, pH 7.26) and stored at 4 °C. The concentration of CT-DNA was determined by UV absorbance at 260 nm after proper dilution with water, taking 6600 M$^{-1}$ cm$^{-1}$ as the molar absorption coefficient. The ratio of the UV absorbance at 260 and 280 nm ($A_{260}/A_{280}$) was ca 1.8, indicating that the DNA solution was sufficiently free of protein.[6]

CT-DNA (0.1 mM) was incubated alone or with complex **1**, **2**, **3**, or **4** (0.1 mM) in the buffer (5 mM Tris-HCl/50 mM NaCl, pH 7.26) at 37 °C for 12 h. CD spectra were recorded at room temperature in the wavelength range of 220−320 nm. Three scans were performed for each spectrum.

The fluorescence of the EB-DNA system was determined in the buffer (5 mM Tris-HCl/50 mM NaCl, pH 7.26) at room temperature ($\lambda_{ex}$ = 520 nm; $\lambda_{em}$ = 610 nm). Specifically, the CT-DNA solution (25 $\mu$L, 0.45 mM) was added to the EB buffer (3 mL). Aliquots of the complex solution (2.6, 2.54, 1.65, and $1.72 \times 10^{-4}$ M for **1**−**4**, respectively) were then added to the EB-DNA solution, and the fluorescence was measured after each addition until a 50% reduction of fluorescence appeared. The apparent binding constant ($K_{app}$) was calculated using the equation

$$K_{EB}[EB] = K_{app}[complex]$$

where $K_{EB} = 1.0 \times 10^7$ M$^{-1}$, [EB] = 1.3 $\mu$M, and [complex] was the final concentration at which a 50% reduction of the fluorescence had occurred.[26]

(25) Price, J. H.; Williamson, A. N.; Schramm, R. F.; Wayland, B. B. *Inorg. Chem.* **1972**, *11*, 1280–1284.
(26) Lee, M.; Rhodes, A. L.; Wyatt, M. D.; Forrow, S.; Hartley, J. A. *Biochemistry* **1993**, *32*, 4237–4245.

**Scheme 1.** Synthetic Route of the Ligands

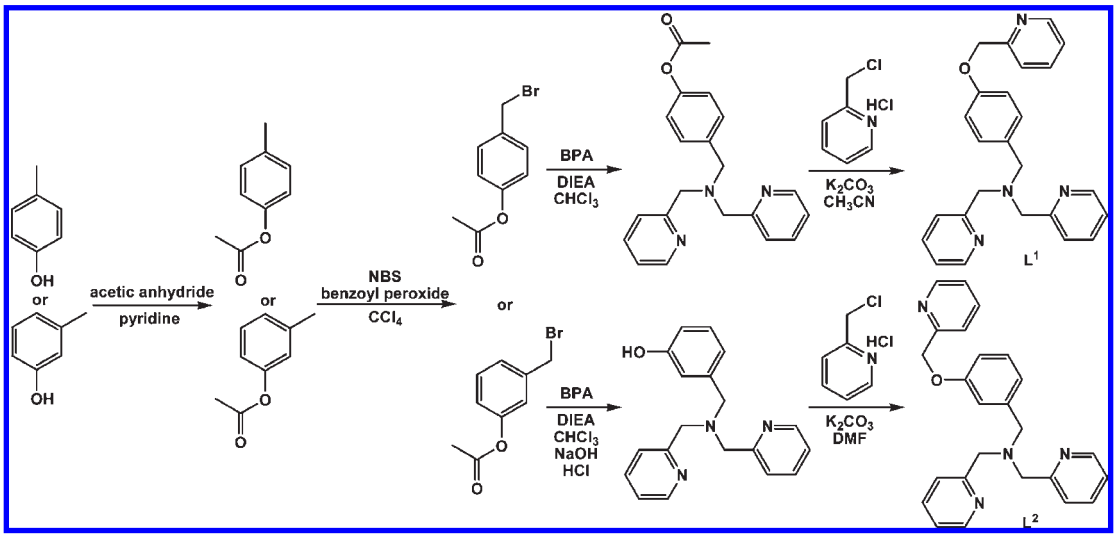


UV−vis absorption titration was carried out by adding different concentrations of the CT-DNA solution to the complex solutions with constant concentration. The changes of the absorption intensity with increasing concentrations of CT-DNA were recorded after equilibrium. The intrinsic binding constant $K_b$ of the complexes to CT-DNA was obtained by regression analysis using the equation

$$(\varepsilon_a - \varepsilon_f)/(\varepsilon_b - \varepsilon_f) = [b - (b^2 - 2K_b{}^2 C_t[\mathrm{DNA}]/s)^{1/2}]/2K_b C_t$$

where $b = 1 + K_b C_t + K_b[\mathrm{DNA}]/2s$, $\varepsilon_a$, $\varepsilon_f$, and $\varepsilon_b$ are the extinction coefficients of the charge-transfer absorption band at a given DNA concentration, of the free complex in solution, and of the DNA-bound complex, respectively, $C_t$ is the total complex concentration, [DNA] is the DNA concentration in nucleotides, and $s$ is the binding site size in base pairs.[27] The nonlinear least-squares analysis was finished using *Origin 8.0*.

**Agarose Gel Electrophoresis.** The DNA binding ability of the complexes was tested by treating supercoiled pUC19 DNA (200 ng) with gradient concentrations of the complex in the buffer (50 mM Tris-HCl/50 mM NaCl, pH 7.4) until the total volume reached 10 $\mu$L. The mixtures were incubated at 37 °C for 12 h, and the reactions were quenched by 2 $\mu$L of loading buffer (30 mM EDTA, 36% glycerol, 0.05% xylene cyanol FF, and 0.05% bromophenol blue). The resulting solutions were loaded onto the agarose gel (1%) and subjected to electrophoresis in a TAE buffer (40 mM Tris acetate and 1 mM EDTA). DNA bands were stained by EB, visualized under UV light, and photographed.

The DNA cleavage experiments were carried out in a method similar to that described above except that ascorbic acid (Vc; 1 $\mu$L) at a 100-fold molar concentration of each complex was added to the reaction system as an initiator and the incubation time was shortened to 1 h. The quantification of each DNA form was accomplished by densitometric analysis on the agarose gel containing EB. A correction factor of 1.47 was used for the supercoiled DNA (form I) assessment because intercalation of EB to form I DNA is relatively weak as compared to that of nicked (form II) and linear DNA (form III).[28] The fraction of each DNA form was defined as the ratio of the individual band intensity to total band intensity in a specific lane. The reported results are the mean value of the triplicate experiments.

**Analysis of ROS.** Common radical scavengers like $NaN_3$ (1 $\mu$L, 1 M), KI (1 $\mu$L, 1 M), and dimethyl sulfoxide (DMSO; 1 $\mu$L, 100%) were added to the buffer solutions (50 mM Tris-HCl/50 mM NaCl, pH 7.4) containing supercoiled pUC19 DNA (200 ng) prior to the addition of each complex (1 $\mu$L, 20 $\mu$M), respectively. The mixture was incubated at 37 °C for 10 min, and Vc (1 $\mu$L, 10 mM) was added to initiate the reaction ($V_{total}$, 10 $\mu$L). The subsequent quench, electrophoresis, and quantification procedures were performed as described above.

## Results and Discussion

**Design and Synthesis.** Two multidentate ligands $L^1$ and $L^2$ were designed to satisfy the coordination of copper(II) and platinum(II) centers simultaneously (Scheme 1). Copper(II) complexes **1** and **2** were obtained directly from the reaction of $L^1$ or $L^2$ with $CuCl_2 \cdot 2H_2O$ in methanol at room temperature, and heterodinuclear complexes **3** and **4** were prepared by the reaction of *cis*-$[Pt(DMSO)_2Cl_2]$ with **1** or **2** in methanol, respectively. The linkers between copper(II) and platinum(II) centers in **3** and **4** are rigid *p*- and *m*-cresol, respectively. The platinum(II) center in these complexes is coordinated to a 2-methylpyridine, a DMSO, and two chloride ligands. According to the configuration of $[Pt(DMSO)_2Cl_2]$,[25] the chlorides are most likely in a cis conformation. The copper(II) center comprises a BPA and two chloride ligands, which was proven to be an effective DNA scission motif in our previous study.[13] In this design, complexes **3** and **4** are expected to combine the selective binding ability of the *cis*-platinum moiety with the cleavage property of the Cu-BPA component. Considering the preference of the *cis*-dichloroplatinum moiety for the N7 position of neighboring adenine and/or guanine in the major groove of DNA,[29,30] the platinum moiety in **3** and **4** may selectively direct the copper part to the GG or AG site (vide infra).

**Characterization of the Complexes.** The formation of metal complexes and the speciation of various ionic forms in a methanol solution were studied with ESI-MS.

(27) Lahiri, D.; Bhowmick, T.; Pathak, B.; Shameema, O.; Patra, A. K.; Ramakumar, S.; Chakravarty, A. R. *Inorg. Chem.* **2009**, *48*, 339–349.
(28) Jin, Y.; Cowan, J. A. *J. Am. Chem. Soc.* **2005**, *127*, 8408–8415.
(29) Cepeda, V.; Fuertes, M. A.; Castilla, J.; Alonso, C.; Quevedo, C.; Pérez, J. M. *Anti-Cancer Agents Med. Chem.* **2007**, *7*, 3–18.
(30) Temple, M. D.; McFadyen, W. D.; Holmes, R. J.; Denny, W. A.; Murray, V. *Biochemistry* **2000**, *39*, 5593–5599.

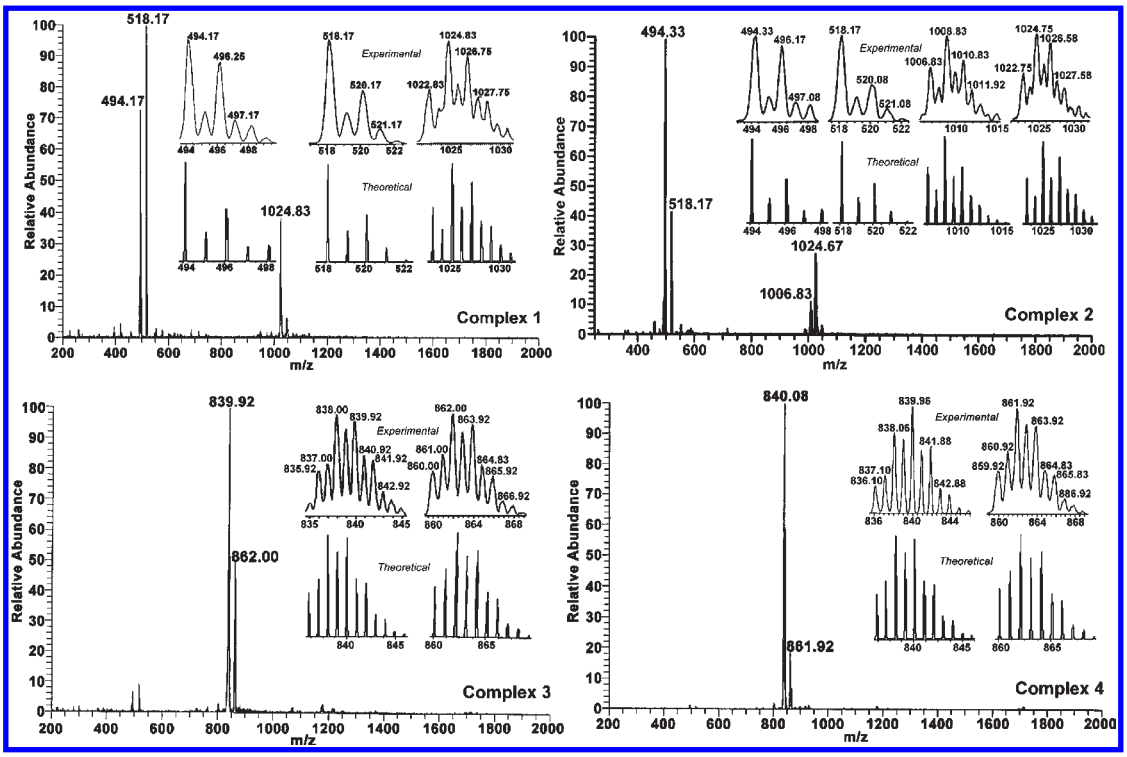


**Figure 2.** ESI-MS spectra of complexes **1**−**4** in a methanol solution. Insets are the determined isotopic distribution patterns and the corresponding simulated ones of the observed peaks.

**Table 1.** Assignment of the Major Observed Peaks in the ESI-MS Spectra for Complexes **1**−**4** (See Figure 2)

| complex | species | formula | obsd *m*/*z* | calcd *m*/*z* |
|---|---|---|---|---|
| **1** | $[\mathbf{1} - Cl]^+$ | $C_{25}H_{24}ClCuN_4O$ | 494.17−498.25 | 494.10 |
| | $[\mathbf{1} - 2Cl + CH_3COO^a]^+$ | $C_{27}H_{27}CuN_4O_3$ | 518.17−522.08 | 518.14 |
| | $[\mathbf{1}\cdot(\mathbf{1} - Cl)]^+$ | $C_{50}H_{48}Cl_3Cu_2N_8O_2$ | 1024.83−1030.67 | 1025.18 |
| **2** | $[\mathbf{2} - Cl]^+$ | $C_{25}H_{24}ClCuN_4O$ | 494.33−498.17 | 494.10 |
| | $[\mathbf{2} - 2Cl + CH_3COO]^+$ | $C_{27}H_{27}CuN_4O_3$ | 518.17−522.08 | 518.14 |
| | $[(\mathbf{2} - Cl)_2 + OH]^+$ | $C_{50}H_{49}Cl_2Cu_2N_8O_3$ | 1006.83−1014.92 | 1006.21 |
| | $[\mathbf{2}\cdot(\mathbf{2} - Cl)]^+$ | $C_{50}H_{48}Cl_3Cu_2N_8O_2$ | 1024.67−1030.67 | 1025.18 |
| **3** | $[\mathbf{3} - Cl]^+$ | $C_{27}H_{30}Cl_3CuN_4O_2PtS$ | 835.92−843.83 | 840.04 |
| | $[\mathbf{3} - 2Cl + CH_3COO]^+$ | $C_{29}H_{33}Cl_2CuN_4O_4PtS$ | 860.00−867.92 | 862.07 |
| **4** | $[\mathbf{4} - Cl]^+$ | $C_{27}H_{30}Cl_3CuN_4O_2PtS$ | 836.10−843.86 | 840.04 |
| | $[\mathbf{4} - 2Cl + CH_3COO]^+$ | $C_{29}H_{33}Cl_2CuN_4O_4PtS$ | 859.92−867.83 | 862.07 |

[a] $CH_3COO^-$ was introduced by an eluent that contains a trace amount of $CH_3COOH$.

As Figure 2 shows, three major peaks are observed at *m*/*z* 494.17, 518.17, and 1024.83 for complex **1**, which could be assigned to $[\mathbf{1} - Cl]^+$, $[\mathbf{1} - 2Cl + CH_3COO]^+$, and $[\mathbf{1}\cdot(\mathbf{1} - Cl)]^+$, respectively. Complex **2** also presents three major peaks at *m*/*z* 494.33, 518.17, and 1024.67, which could be attributed to $[\mathbf{2} - Cl]^+$, $[\mathbf{2} - 2Cl + CH_3COO]^+$, and $[\mathbf{2}\cdot(\mathbf{2} - Cl)]^+$, respectively. Complex **3** has two major peaks at *m*/*z* 839.92 and 862.00, which correspond to $[\mathbf{3} - Cl]^+$ and $[\mathbf{3} - 2Cl + CH_3COO]^+$, respectively. Two peaks assignable to $[\mathbf{4} - Cl]^+$ and $[\mathbf{4} - 2Cl + CH_3COO]^+$ are observed at *m*/*z* 840.08 and 861.92 for complex **4**, but the latter peak is rather weak. The isotopic distribution patterns of the above peaks match well with the theoretical results simulated by the *Isopro 3.0* program. The detailed assignments of the peaks observed in the spectra are listed in Table 1. ESI-MS observations indicate that the metal-ligated skeletons of these complexes are stable in solution and the chloride ligand may dissociate from the complex. This suggests that the complexes could covalently bind to DNA after losing the labile $Cl^-$.

The complexes were further characterized by IR spectra and elemental analysis. The vibration bands for Cu−Cl (267.2−274.8 $cm^{-1}$), Pt−Cl (311.9−339.9 $cm^{-1}$), and Pt−S (438.3−440.4 $cm^{-1}$) can be clearly observed in the far-IR spectra (see Figure S1 in the Supporting Information),[31,32] and the results of elemental analysis fit well the composition of the complexes. The involvement of a *cis*-$[Pt(DMSO)Cl_2]$ unit in complexes **3** and **4** is also demonstrated by the $^1H$ NMR spectra (see Figure S2 in the Supporting Information), where the picolin protons were downfield-shifted when the copper complexes reacted with *cis*-$[Pt(DMSO)_2Cl_2]$.

(31) Whyman, R.; Hatfield, W. E. *Inorg. Chem.* **1967**, *6*, 1859–1862.
(32) Marqués-Gallego, P.; den Dulk, H.; Brouwer, J.; Kooijman, H.; Spek, A. L.; Roubeau, O.; Teat, S. J.; Reedijk, J. *Inorg. Chem.* **2008**, *47*, 11171–11179.

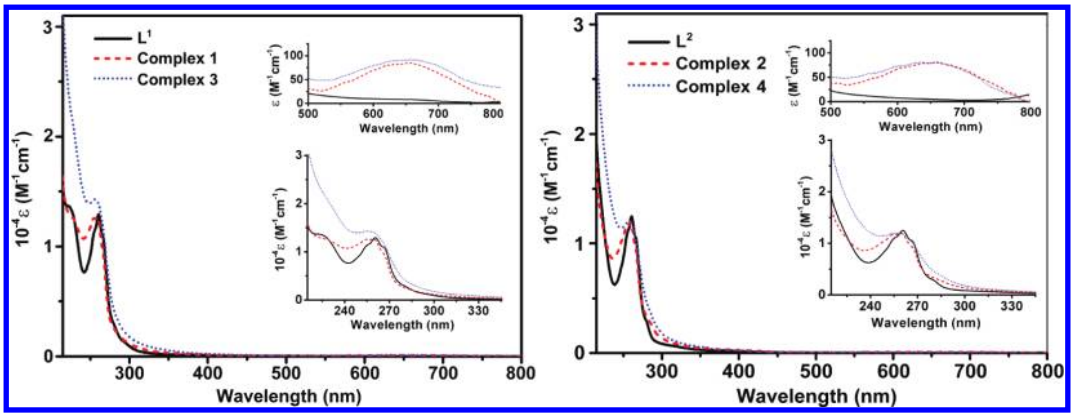


**Figure 3.** UV−vis spectra of $L^1$, $L^2$, and complexes **1**−**4** (0.1 M) in an aqueous solution. Insets show closeups of the $\pi \rightarrow \pi^*$ (240−280 nm) and d−d (550−750 nm) absorption features.

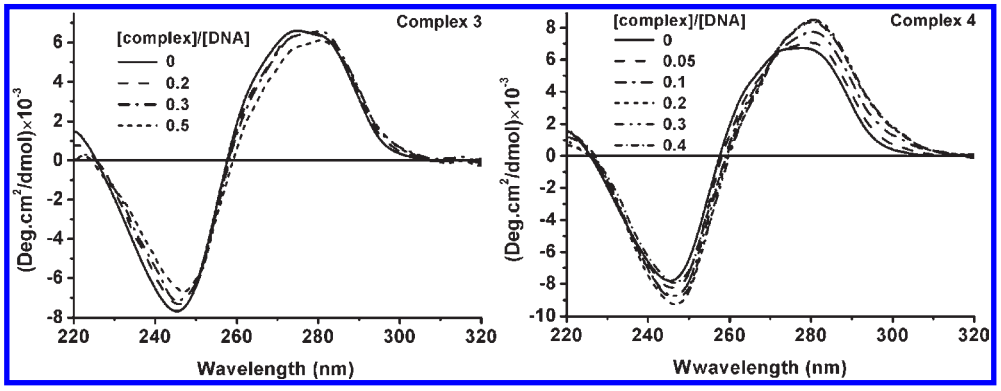


**Figure 4.** CD spectra of CT-DNA (0.1 mM) in the presence of complexes **3** and **4**, respectively, at different [complex]/[DNA] molar ratios.

Characterization of the complexes in aqueous solutions was investigated by UV−vis spectroscopy. As shown in Figure 3, ligand $L^1$ shows an intense absorption band at ca. 260 nm and two shoulder bands at around 260 nm, which could be assigned to the n $\rightarrow \pi^*$ and $\pi \rightarrow \pi^*$ absorption bands of pyridyls. The spectrum of copper(II) complex **1** is similar to that of $L^1$ except that the absorption band at 260 nm is flattened and a broad weak d−d absorption band appears in the region of 550−750 nm because of copper(II) coordination with pyridyls.[23,33] The formation of complex **3** from **1** barely influences the weak d−d absorption band but further broadens the $\pi \rightarrow \pi^*$ absorption band at 260 nm because one more pyridyl is involved in the coordination with platinum(II). The spectral features of ligand $L^2$ and complexes **2** and **4** are similar to those of ligand $L^1$ and complexes **1** and **3**. These results demonstrate that copper(II) remains bound to the pyridyls in solution and in the presence of platinum(II).

**DNA Binding Behavior of the Complexes.** CD spectroscopy was used to probe the global changes in the DNA conformation induced by the complexes. The CD spectra of CT-DNA exhibit a positive band at 275 nm due to the base stacking and a negative band at 245 nm due to the helicity, which is characteristic of B-DNA.[34] With the addition of complex **1** or **2**, the CD spectra only show a slight change in the ellipticity for both positive and negative bands (see Figure S3 in the Supporting Information), suggesting that **1** and **2** may interact with CT-DNA chiefly in an electrostatic mode.[35] Complexes **3** and **4** perturb the base stacking and helicity bands more considerably than **1** and **2** (Figure 4). For complex **3**, both positive and negative bands display a decrease in the ellipticity and a slight red shift in the maximum wavelength when the molar ratio of the complex to CT-DNA (*r*) progressively increases. This is an indication of B $\rightarrow$ Z conformational conversion, though limited, with increased winding of the DNA helix through rotation of the bases.[36] Apparently, the decrease in the ellipticity of the CD band is mainly induced by the platinum moiety, which has been related to the formation of short single-stranded segments containing unpaired bases.[37] For complex **4**, the ellipticity of both bands increases with respect to free DNA when the *r* value is less than 0.4; however, it begins to decrease when the ratio reaches 0.4. The change of the positive band is similar to that induced by cisplatin,[38,39] which may reflect the contribution of the *cis*-platinum moiety to the

(33) Karlin, K. D.; Cohen, B. I. *Inorg. Chim. Acta* **1985**, *107*, L17–L20.
(34) Johnson, W. C. In *Circular Dichroism: Principles and Applications*; Nakanishi, K., Berova, N., Woody, R. W., Eds.; VCH: New York, 1994; pp 523−540.
(35) Tang, S.-P.; Hou, L.; Mao, Z.-W.; Ji, L.-N. *Polyhedron* **2009**, *28*, 586–592.
(36) Moradell, S.; Lorenzo, J.; Rovira, A.; Robillard, M. S.; Avilés, F. X.; Moreno, V.; de Llorens, R.; Martinez, M. A.; Reedijk, J.; Llobet, A. *J. Inorg. Biochem.* **2003**, *96*, 493–502.
(37) Žaludová, R.; Žákovská, A.; Kašpárková, J.; Balcarová, Z.; Kleinwächter, V.; Vrána, O.; Farrell, N.; Brabec, V. *Eur. J. Biochem.* **1997**, *246*, 508–517.
(38) Gay, M.; Montaña, Á. M.; Moreno, V.; Prieto, M.-J.; Llorens, R.; Ferrer, L. *J. Inorg. Biochem.* **2005**, *99*, 2387–2394.
(39) Gay, M.; Montaña, A. M.; Moreno, V.; Prieto, M.-J.; Pérez, J. M.; Alonso, C. *Bioorg. Med. Chem.* **2006**, *14*, 1565–1572.

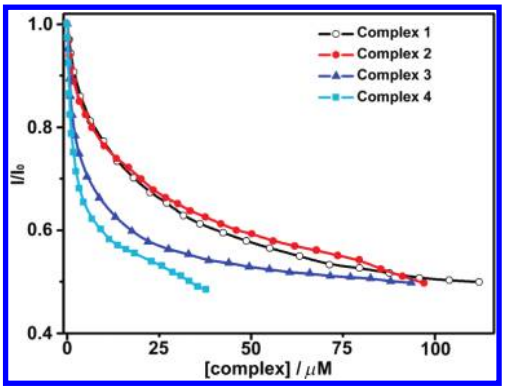


**Figure 5.** Fluorescence decrease ($\lambda_{em}$ = 520 nm) induced by complexes **1**−**4** through the displacement of CT-DNA-bound ethidium bromide in the buffer (5 mM Tris-HCl/50 mM NaCl, pH 7.26).

modification of the secondary structure of DNA. In contrast with cisplatin, the intensity of the negative band also increases simultaneously as compared with that of free DNA, which may result from the influence of the Cu-BPA component. In general, the major feature of the spectra is the increase in the ellipticity for both bands of CT-DNA, which is an indication of a typical intercalation involving $\pi-\pi^*$ stacking and stabilization of the right-handed B form of CT-DNA.[40,41] The CD spectra demonstrate that copper(II) complexes **1** and **2** exert only a small influence on the DNA conformation, while copper(II)−platinum(II) complexes **3** and **4** have a more evident impact on the conformation of DNA. The interaction mode of these two types of complexes with DNA is different, where the platinum(II) center plays a crucial role. Nevertheless, the geometry of the ligands also affects the interaction, which is evidenced by the spectral difference between **3** and **4**. According to the changes in ellipticity induced by these complexes, their perturbation on the base-stacking and helicity bands of CT-DNA follows an order of **1** < **2** < **3** < **4**.

The DNA binding behavior of the complexes was further investigated using the EB-DNA system. EB is an intercalator that gives a significant increase in the fluorescence emission when bound to DNA, and its displacement from DNA results in a decrease in the emission intensity.[42] The apparent DNA binding constants ($K_{app}$) of the four complexes were thus determined by the EB displacement assay.[26] As Figure 5 shows, the fluorescence intensity ($I$) of the EB-DNA system at 610 nm decreases remarkably with the addition of the complex, suggesting that the complex can replace the DNA-bound EB and the binding mode involves some intercalative interaction. However, the binding propensity of these complexes is different. On the basis of the titration profiles, $K_{app}$ of complexes **1**−**4** is calculated as $1.16 \times 10^5$, $1.34 \times 10^5$, $1.47 \times 10^5$, and $3.42 \times 10^5$ $M^{-1}$, respectively. The results are in accordance with the above CD observations.

The intrinsic binding constant ($K_b$) of complexes **3** and **4** to CT-DNA was determined by UV−vis absorption titration and the subsequent regression analysis. As Figure 6 presents, upon the addition of an increasing amount of CT-DNA to a solution of the complex, an apparent hypochromism and a slight red shift (1.5−2 nm) were observed near 260 nm, which is generally assigned to the intercalation involving stacking interactions between the aromatic chromophores and the base pairs of DNA.[43] The $K_b$ values of complexes **3** and **4** obtained from the regression analysis are $4.5 \times 10^4$ and $6.9 \times 10^4$ $M^{-1}$, respectively. These results suggest that both complexes **3** and **4** can bind to CT-DNA moderately, and **4** is somewhat better than **3** for DNA binding, which agrees with the above results obtained from other experiments.

The binding of complexes **3** and **4** to DNA was confirmed additionally with agarose gel electrophoresis. As Figure 7 shows, the migration rate of the supercoiled DNA (form I) is retarded and the amount of the nicked DNA (form II) is increased after pUC19 DNA was incubated with the complexes, which indicates that the complexes can induce the unwinding of the DNA superhelix. Simultaneously, the mobility of form II DNA is slightly accelerated, which may be due to the binding of the *cis*-platinum moiety to DNA shortens and condenses the helix.[44] The separation between forms I and II narrows as the concentration of the complex increases. The bands of forms I and II coalesce into one when the concentration reaches 100 $\mu$M for complex **3** (part a, lane 5) and 60 $\mu$M for complex **4** (part b, lane 6), respectively. This coalescence point corresponds to the amount of the complex that is necessary for the complete removal of form I DNA. Beyond this point, the migration rate begins to increase again as positive supercoils are induced.[45] The results suggest that the DNA binding ability of complex **4** is higher than that of complex **3**, which is consistent with the CD, EB, and UV−vis results discussed above. The discrepancy in the binding ability between **3** and **4** mainly results from the different geometries of their ligands.

The binding sites of the *cis*-platinum moiety in different oligodeoxyribonucleotide duplexes containing GG or AG sequences were studied by Maxam−Gilbert footprinting experiments.[46] Preliminary results indicate that copper(II)−platinum(II) complexes **3** and **4** indeed show some specific binding propensity to GG and AG sequences (see the Supporting Information). However, the binding mode seems more complicated than that of cisplatin analogues in the presence of an additional copper center. For this reason, further investigation is needed to clarify the issue.

**Concentration-Dependent DNA Cleavage Activity.** The DNA cleavage activity of the complexes was studied using supercoiled pUC19 plasmid DNA by gel electrophoresis in the buffer (50 mM Tris-HCl/50 mM NaCl, pH 7.4) under physiologically relevant conditions. Figure 8 shows the electrophoresis results of the DNA cleavage induced by increasing concentrations of the respective complexes in the presence of Vc. All complexes can convert form I DNA into form II at 1 $\mu$M (lanes 3, 7, 11, and 15),

(40) Shahabadi, N.; Kashanian, S.; Purfoulad, M. *Spectrochim. Acta, Part A* **2009**, *72*, 757–761.
(41) Efthimiadou, E. K.; Katsaros, N.; Karaliota, A.; Psomas, G. *Inorg. Chim. Acta* **2007**, *360*, 4093–4102.
(42) Le Pecq, J. B.; Paoletti, C. *J. Mol. Biol.* **1967**, *27*, 87–106.
(43) Baldini, M.; Belicchi-Ferrari, M.; Bisceglie, F.; Dall'Aglio, P. P.; Pelosi, G.; Pinelli, S.; Tarasconi, P. *Inorg. Chem.* **2004**, *43*, 7170–7179.
(44) Zhao, Y. M.; He, W. J.; Shi, P. F.; Zhu, J. H.; Qiu, L.; Lin, L. P.; Guo, Z. J. *Dalton Trans.* **2006**, 2617–2619.
(45) Keck, M. V.; Lippard, S. J. *J. Am. Chem. Soc.* **1992**, *114*, 3386–3390.
(46) Comess, K. M.; Costello, C. E.; Lippard, S. J. *Biochemistry* **1990**, *29*, 2102–2110.

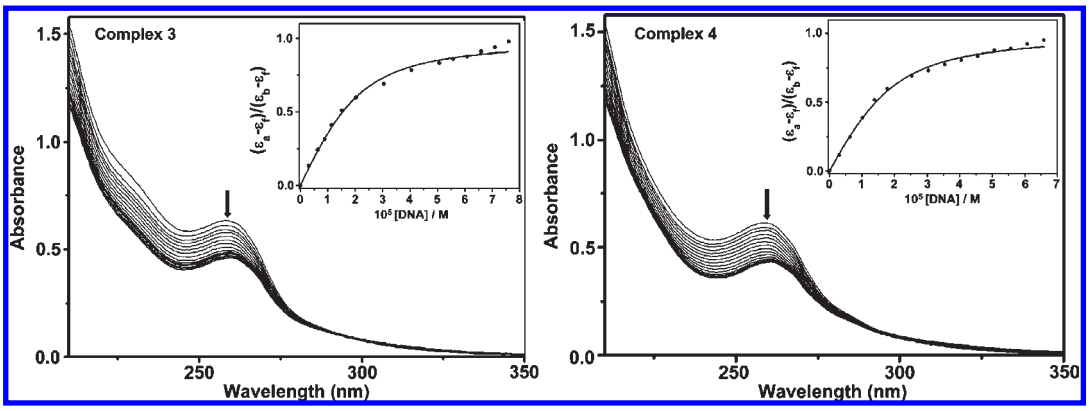


**Figure 6.** UV−vis spectral variations of complexes **3** (45 $\mu$M) and **4** (50.7 $\mu$M) during titration with increasing concentrations of CT-DNA in the buffer (5 mM Tris-HCl/50 mM NaCl, pH 7.26). Insets show the least-squares fit of $(\varepsilon_a - \varepsilon_f)/(\varepsilon_b - \varepsilon_f)$ vs [DNA] for the complexes.

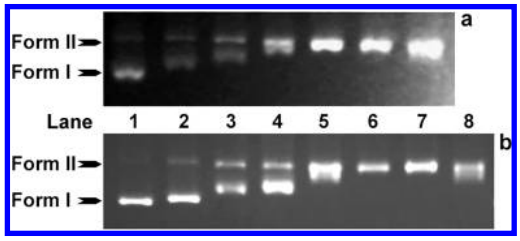


**Figure 7.** Agarose gel electrophoresis patterns of supercoiled pUC19 plasmid DNA (200 ng) incubated with complex **3** (a) or **4** (b) in the buffer (50 mM Tris-HCl/50 mM NaCl, pH 7.4) at 37 °C for 12 h. (a) Lane 1, DNA control; lanes 2−7, DNA + **3** (25, 50, 75, 100, 125, and 150 $\mu$M, respectively). (b) Lane 1, DNA control; lanes 2−8, DNA + **4** (20, 30, 40, 50, 60, 70, and 80 $\mu$M, respectively).

and **2** seems more active (lane 7) than the others at this concentration. Linear DNA (form III) appears at 5 $\mu$M for **1** and **2** (lanes 4 and 8) and at 2.5 $\mu$M for **3** and **4** (lanes 12 and 16). At 10 $\mu$M, complexes **1**−**3** cleave 79.5%, 94.5%, and 95.6% of form I DNA and the percentages of form III DNA reach 2.6%, 10.3%, and 23.1% (lanes 5, 9, and 14), respectively. At the same concentration, complex **4** completely cleaves form I DNA into forms II and III DNA (lane 18). At 20 $\mu$M, form I DNA is totally transformed into forms II and III DNA for complex **2** (lane 10), but it is still observable for complex **1** (lane 6). The most impressive cleavage feature observed for these complexes is that form III DNA appears before the disappearance of form I DNA (lanes 4−6, 8, 9, 12−14, 16, and 17). This phenomenon indicates that the complexes are capable of performing direct double-strand scission,[17] while many copper complexes are only able to cleave single strand successively.

The above results demonstrate that all of the complexes designed in this study have remarkable cleavage activity, particularly complexes **3** and **4**, which show higher activity than **1** and **2** at most corresponding concentrations. A synergistic effect between the copper(II) and platinum(II) centers may exist in **3** and **4**. Because the ligands of the correlated complexes (**1** vs **3** and **2** vs **4**) and the structures of the copper(II) moieties are identical, the superior cleavage activity of **3** and **4** manifestly indicates that the introduction of an additional platinum(II) center to the copper(II) complex can significantly enhance the nuclease efficiency. The geometry of the ligands also influences the cleavage activity. For complexes containing the same metal center or centers (**1** vs **2** and **3** vs **4**), *m*-cresol-derived compounds are more active than their *p*-cresol-derived counterparts. However, this influence could be overshadowed by the impact of the metal core. Considering all of these factors, a comprehensive order in terms of the nuclease activity could be concluded as **1** < **2** < **3** < **4**.

**Time-Dependent DNA Cleavage Activity.** The time course of pUC19 DNA cleavage mediated by the complexes (10 $\mu$M) was followed with agarose gel electrophoresis in the buffer (50 mM Tris-HCl/50 mM NaCl, pH 7.4) at 37 °C. As shown in Figure 9, for complexes **1** and **2**, the major cleavage product is form II DNA, which accounts for ca. 80% of the total DNA during the whole time, while form III DNA remains small (< 15%) within 90 min (lanes 3−10). For complexes **3** and **4**, form II DNA is relatively low (ca. 60−70%) in the cleavage products as compared with that for **1** and **2**, while form III DNA displays an ever-increasing trend in the testing time (lanes 11−18). At 10 min, **1** and **2** convert under 3% of the total DNA to form III (lanes 3 and 7), while **3** and **4** convert over 10% and 20% of the total DNA to form III, respectively (lanes 11 and 15). At 30 min, complexes **1** and **2** only transform ca. 5% of the supercoiled DNA into form III DNA (lanes 4 and 8), but complexes **3** and **4** achieve over 20% (lanes 12 and 16). At 60 min, form I DNA is completely converted into forms II and III DNA by **3** and **4** (lanes 13 and 17), whereas it is still detectable even at 90 min in the case of **1** and **2** (lanes 6 and 10). Around 40% of the supercoiled DNA is converted into form III DNA by complexes **3** and **4** at 90 min (lanes 14 and 18). Taken together, the cleavage efficiency is similar between the same type of complexes, i.e., **1** vs **2** and **3** vs **4**, with that of **2** and **4** being somewhat higher than that of **1** and **3**, respectively. However, the superiority of copper(II)−platinum(II) complexes to copper(II) complexes is notable, in that the cleavage efficiency of **3** and **4** is head and shoulders above that of **1** and **2** during the entire time course. These results lead to the same conclusion as that obtained from the concentration dependent data, that is, the cleavage efficiency of the complexes follows an order of **1** < **2** < **3** < **4**. The promotive effect of the platinum(II) center on the DNA cleavage activity of copper(II) complexes is thus confirmed by these experiments.

**ROS Responsible for DNA Cleavage.** In order to identify the ROS that are responsible for the DNA cleavage

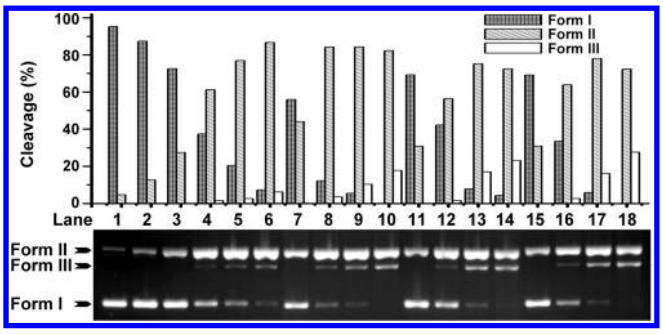


**Figure 8.** Agarose gel electrophoresis patterns of pUC19 plasmid DNA (200 ng) after incubation with Vc (1 mM) and each complex in the buffer (50 mM Tris-HCl/50 mM NaCl, pH 7.4) at 37 °C for 1 h. Lane 1, DNA control; lane 2, DNA + Vc; lanes 3−6, DNA + Vc + **1** (1, 5, 10, and 20 $\mu$M); lanes 7−10, DNA + Vc + **2** (1, 5, 10, and 20 $\mu$M); lanes 11−14, DNA + Vc + **3** (1, 2.5, 5, and 10 $\mu$M); lanes 15−18, DNA + Vc + **4** (1, 2.5, 5, and 10 $\mu$M).

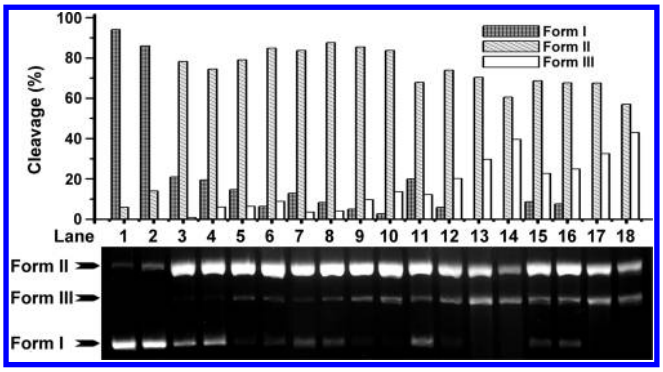


**Figure 9.** Agarose gel electrophoresis patterns of pUC19 plasmid DNA (200 ng) after incubation with each complex (10 $\mu$M) and Vc (1 mM) in the buffer (50 mM Tris-HCl/50 mM NaCl, pH 7.4) at 37 °C for 10, 30, 60, and 90 min, respectively. Lane 1, DNA control; lane 2, DNA + Vc; lanes 3−6, DNA + **1** + Vc; lanes 7−10, DNA + **2** + Vc; lanes 11−14, DNA + **3** + Vc; lanes 15−18, DNA + **4** + Vc.

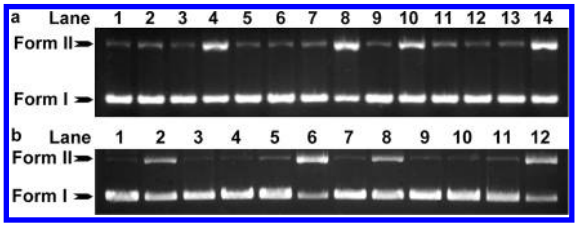


**Figure 10.** Agarose gel electrophoresis patterns of pUC19 plasmid DNA (200 ng) after incubation with each complex (2 $\mu$M) and Vc (1 mM) for 1 h at 37 °C in the absence or presence of different scavengers. (a) Lane 1, DNA control; lane 2, DNA + Vc; lane 3, DNA + **1**; lane 4, DNA + **1** + Vc; lanes 5−8, DNA + **1** + Vc + S; lane 9, DNA + **3**; lane 10, DNA + **3** + Vc; lanes 11−14, DNA + **3** + Vc + S. (b) Lane 1, DNA + **2**; lane 2, DNA + **2** + Vc; lanes 3−6, DNA + **2** + Vc + S; lane 7, DNA + **4**; lane 8, DNA + **4** + Vc; lanes 9−12, DNA + **4** + Vc + S. S stands for scavenger DMSO (10%), KI (100 mM), $NaN_3$ (100 mM), and $D_2O$ (70%) sequentially in each group of lanes.

reaction, experiments in the presence of different common scavengers such as $NaN_3$, KI, and DMSO were carried out, respectively. As Figures 10 and 11 present, the cleavage activity of **1**−**4** is reduced dramatically by the presence of hydroxyl radical scavenger DMSO (lanes a5, b3, a11, and b9), indicating that diffusible $^{\bullet}OH$ plays a key

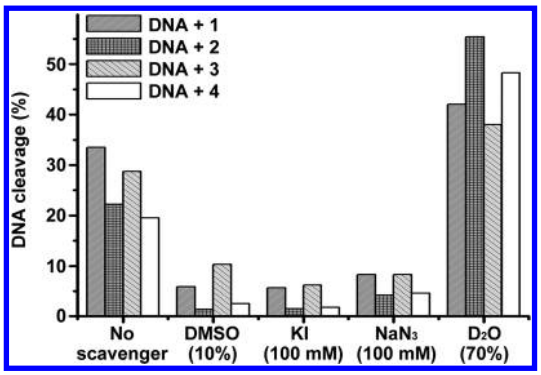


**Figure 11.** Histogram showing the influence of different radical scavengers on the scission of supercoiled pUC19 DNA (200 ng) by complexes **1**−**4** (2 $\mu$M), respectively, in the presence of Vc (1 mM) after incubation at 37 °C for 1 h.

role in the cleavage process. Hydrogen peroxide scavenger KI also markedly inhibits the cleavage activity of the complexes (lanes a6, b4, a12, and b10), suggesting that $H_2O_2$ is involved in the cleavage reaction. Singlet oxygen scavenger $NaN_3$ significantly diminishes the cleavage activity of the complexes (lanes a7, b5, a13, and b11), suggesting that $^1O_2$ also takes part in the cleavage mechanism. The involvement of $^1O_2$ is also demonstrated by the remarkable enhancement of the cleavage activity in $D_2O$ (lanes a8, b6, a14, and b12), where the lifetime of $^1O_2$ is significantly longer than that in water.[27] In summary, these complexes seem to follow some similar pathways in the cleavage process, in which hydroxyl radicals, hydrogen peroxide, and singlet oxygen are crucial ROS for the cleavage reactions.

## Conclusion

Heteronuclear complexes containing copper(II) and platinum(II) centers have displayed some intriguing nuclease properties. The combination of a site-specific group and a scission moiety may enhance the regional selectivity and cleavage efficiency of an artificial nuclease. As compared with the corresponding copper(II) complexes, the heteronuclear complexes synthesized in this work exhibit an enhanced DNA binding ability and a superior cleavage activity because of the preferential affinity of platinum(II) for DNA. The geometry of the ligands also has some impact on the cleavage property. These results strongly support the promotive effect of the platinum(II) center in the copper-based nuclease. This work provides a potential approach to achieving a site-specific cleavage of DNA.

**Acknowledgment.** We acknowledge financial support from the National Natural Science Foundation of China (Grants 20631020, 90713001, 20721002, and 30870554) and the Natural Science Foundation of Jiangsu Province (Grant BK2008015).

**Supporting Information Available:** Far-IR, $^1H$ and $^{13}C$ NMR, and CD spectra, details of the Maxam−Gilbert footprinting experiements, and PAGE patterns. This material is available free of charge via the Internet at http://pubs.acs.org.